Preprint. To be published in *Journal of Surface Investigation: X-ray, Synchrotron and Neutron Techniques, 2020, Vol. 14, No. 2.*

Structure of Regions of Regular Motion in the Phase Space of Channeled Electrons

V. V. Syshchenko[a], *, A. I. Tarnovsky[a], A. Yu. Isupov[b], and I. I. Solovyev[a]

[a] *Belgorod State National Research University, Belgorod, 308015 Russia*

[b] *Laboratory of High Energy Physics, Joint Institute for Nuclear Physics, Dubna, 141980 Russia*

**e-mail: syshch@yandex.ru*

Received July 26, 2019; revised August 30, 2019; accepted August 31, 2019

Abstract—The motion of electrons in the axial channeling mode in the [100] direction of a Si crystal can be regular and chaotic (depending on the initial conditions). The contribution of regions of regular and chaotic dynamics to the quasiclassical density of energy levels of the transverse motion of electrons is found in this paper. The obtained values are used as parameters of the Berry—Robnik distribution describing the level spacing statistics in the case of the coexistence of regions of regular and chaotic motion.

Keywords: regular dynamics, chaotic dynamics, quantum chaos, channeling, semiclassical approximation, level spacing statistics, Berry–Robnik distribution

DOI: 10.1134/S1027451020020354

INTRODUCTION

The range of problems of quantum chaos includes the study of the difference between the behaviors of quantum systems having, on the one hand, chaotic dynamics and, on the other hand, regular dynamics [1–4] in the classical limit. The statistical properties of the energy levels of a quantum system are one of the manifestations of quantum chaos that is simplest for analysis. Thus, the distance s between the neighboring energy levels of a chaotic system obeys the Wigner distribution [2–4]:

$$p(s) = (\pi\rho^2 s/2)\exp(-\pi\rho^2 s^2/4), \quad (1)$$

where ρ is the average density of levels in the region of the energy spectra of the system under consideration, while, for systems with regular dynamics, the exponential (Poisson) distribution exists:

$$p(s) = \rho\exp(-\rho s), \quad (2)$$

with a maximum at $s = 0$.

Thus, the tendency to the grouping of energy levels into shells exists in regular systems, while the energy levels exhibit a tendency to mutual repulsion in chaotic systems. Therefore, the manifestations of quantum chaos are more noticeable in the quasiclassical region, where the number of energy levels is large.

The manifestation of dynamic chaos in electron channeling [5, 6] was studied for the case of motion near the [110] direction in a Si crystal in [7–9]. In this case, pairs of neighboring atomic chains produce a double-well potential, above the saddle point of which the motion of electrons turns out to be almost chaotic. It was established that the statistical properties of the levels in this region are described well by the Wigner distribution (1).

The case where the classical dynamics of a particle turns out to be regular at a given energy under certain initial conditions and chaotic under others is more complicated. Such a case occurs, for example, if an electron moves near the [100] direction of a Si crystal [6]. Assuming that, in the quasiclassical limit, the regions of regular motion and the (single) region of chaotic motion generate two independent sequences of levels, Berry and Robnik [10] and also (independently) Bogomolny [11] showed that the distribution of level spacings is described by the following formula:

$$p(s) = \frac{1}{\rho}\exp(-\rho_1 s)\left(\rho_1^2\operatorname{erfc}\left(\pi^{1/2}\rho_2 s/2\right) + \left(2\rho_1\rho_2 + \pi\rho_2^3 s/2\right)\exp\left(-\pi\rho_2^2 s^2/4\right)\right), \quad (3)$$

where ρ_1 and ρ_2 are the densities of levels caused by regular and chaotic dynamics, respectively ($\rho_1 + \rho_2 = \rho$),

$$\operatorname{ercf}(x) = 2\pi^{-1/2}\int_x^\infty \exp(-t^2)dt = 1 - \operatorname{erf}(x).$$

The average density of energy levels of a two-dimensional system in the quasiclassical limit of quantum mechanics is defined by the formula [10]:

$$\rho(E) = (2\pi\hbar)^{-2}\int \delta(E - H(x, y, p_x, p_y))\,dxdydp_xdp_y, \quad (4)$$

where H is the classical Hamiltonian of the system, and the delta function expresses the energy conservation law for the motion of a particle. By integration over p_y, we obtain

$$\rho(E) = 2(2\pi\hbar)^{-2}\int |v_y(x,y,p_x)|^{-1}\,dxdydp_x, \qquad (5)$$

where v_y is the particle velocity component in the direction of the axis y, and integration is performed over the region, determined by the condition

$$p_x^2/2m + U(x,y) \le E. \qquad (6)$$

In this paper, we estimate the contribution ρ_1 and ρ_2 to the average density of nondegenerate energy levels (5); it is based on inclusion of the structure of regions of the regular motion in phase space of an electron moving near the [100] direction of a Si crystal in the axial channeling mode.

EXPERIMENTAL

If the relativistic particle is incident at a small angle ψ to the crystallographic axis closely packed with atoms, then the case where it performs finite motion in the transverse (with respect to the axis) plane, which is called axial channeling, can occur [5, 6]. In this case, the particle motion can be described as motion in the continuous potential of an atomic chain averaged along its length. The particle-momentum component $p_\parallel$, that is parallel to the chain axis is retained in this potential, which makes it possible to describe electron motion in the transverse plane using the two-dimensional Schrödinger equation

$$\widehat{H}\Psi(x,y,t) = i\hbar\frac{\partial}{\partial t}\Psi(x,y,t) \qquad (7)$$

with the Hamilton operator

$$\widehat{H} = -\frac{\hbar^2}{2E_\parallel/c^2}\left(\frac{\partial^2}{\partial x^2}+\frac{\partial^2}{\partial y^2}\right)+U(x,y), \qquad (8)$$

in which the role of the particle mass is played by the quantity $E_\parallel/c^2$, where $E_\parallel = (m^2c^4 + p_\parallel c^2)^{1/2}$ is the energy of longitudinal motion [5].

The continuous potential of an individual atomic chain can be approximated by the formula [5]:

$$U_1(x,y) = -U_0\ln\left(1+\frac{\beta R^2}{x^2+y^2+\alpha R^2}\right), \qquad (9)$$

where $U_0 = 66.6$ eV, $\alpha = 0.48$, $\beta = 1.5$, and $R = 0.194$ Å (the Thomas—Fermi radius) for the Si crystal [100] chain. Such chains form square lattice with a period of $a \approx 1.92$ Å in the (100) plane. The potential electron energy in the chain field is described

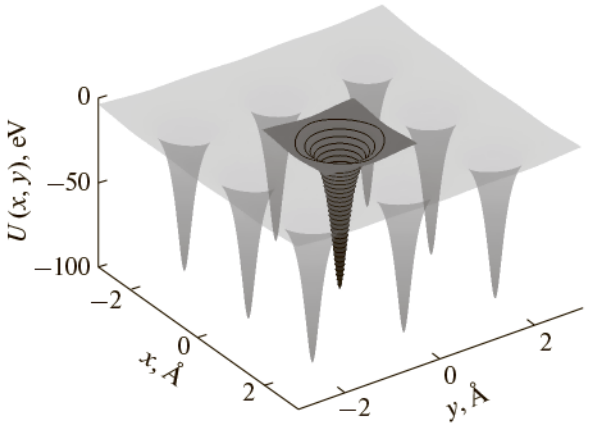

Fig. 1. Potential energy (10) of an electron in the Si crystal [100]-chain field with the inclusion of the contributions of the eight nearest neighbors.

by the following sum if the contributions of its eight nearest neighbors are taken into account:

$$U(x,y) = \sum_{i=-1}^{1}\sum_{j=-1}^{1}U_1(x-ia, y-ja), \qquad (10)$$

the form of this function is given in Fig. 1.

The eigenvalues $E_\perp$ of Hamiltonian (8) with potential (10) (energy levels of the transverse motion of a channeled electron) are found numerically using the so-called spectral method described in [7, 8, 12, 13]. We note that, in the case under consideration, the potential has the symmetry of a square, and all states that are accessible for the particle can be classified by irreducible representations of the group D_4 (or the group C_{4v}, which is isomorphic to it, for example, [14]) depending on the type of wavefunction symmetry. This group has four one-dimensional irreducible representations corresponding to nondegenerate energy levels and one two-dimensional representation corresponding to doubly degenerate levels.

The classical dynamics of the electron in potential (10) was studied by means of the Poincaré section method [3–6]. We remind that the regularity or the chaotic character of particle motion is closely related to the integrability of the equation of motion. If the number of integrals of motion is equal to that of degrees of freedom (up to two in our case), then the system is integrable. In this case, the particle trajectory in phase space lies on the surface

$$E_\perp = H(x,y,p_x,p_y), \qquad (11)$$

having the topological properties of a torus. In this case, the motion turns out to be regular (periodic or quasiperiodic). In the opposite case, the motion is chaotic.

The Poincaré section method makes it possible to clarify whether the system has another (together with the energy) integral of motion. In this method, all

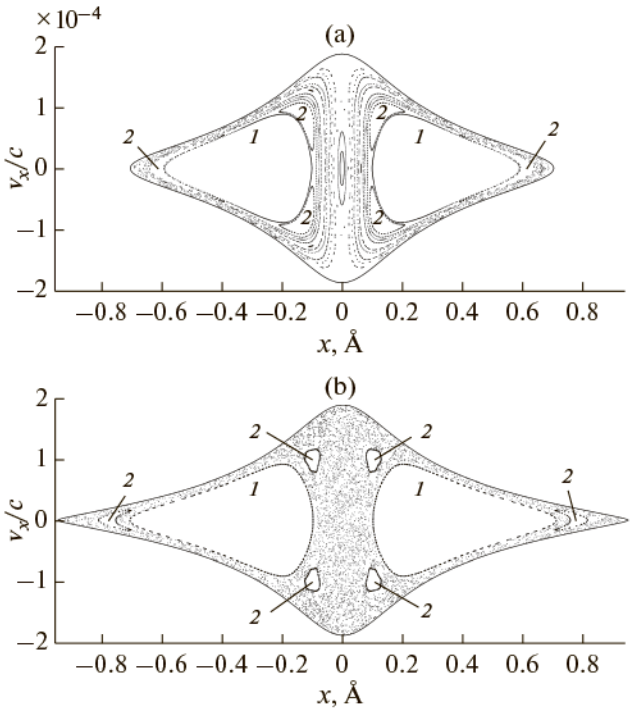

Fig. 2. Poincaré sections for (a) $E_\perp = -14$ eV and (b) $E_\perp = -12.0885$ eV of an electron with an energy of $E_\parallel = 5$ GeV moving in potential (10).

points of intersection of the trajectory with any plane, for example, with the plane (x, p_x) in phase space, are recorded in the process of numerical simulation of the particle trajectory. If the following integral of motion

$$J = J(x, y, p_x, p_y), \qquad (12)$$

exists together with the energy, then, under the condition $y = 0$, we obtain the relation between the variables x and p_x. excluding the variable p_y from Eqs. (11) and (12). In this case, the recorded points lie on a smooth curve in the Poincaré graph (Fig. 2). In the case of the absence of a second integral of motion, the points lie chaotically within the limits of some region (as, for example, in Fig. 2b).

The contribution of the regions of regular motion to the total density of levels (4) was estimated as follows. When calculating integral (5) by means of the Monte Carlo method, random points (x, y, p_x), within the region allowed for motion (6), were considered as the initial points of the phase trajectories, each of which was traced up to the intersection with the plane (x, p_x). In the case where the intersection point fell within the region of regular motion at the Poincaré intersection, the contribution of the corresponding initial point was taken into account not only in the total level density ρ, but also in the density ρ_1, corresponding to regular motion. We emphasize that, for the given initial point (x, y, p_x), two possibilities of choosing the sign of the velocity component along axis y exist:

$$v_y = \pm\left[2c^2\left(E_\perp - U(x, y) - c^2/2E_\parallel\right)/E_\parallel\right]^{1/2}. \qquad (13)$$

However, the presence of these two possibilities was already taken into account when passing from (4) to (5); therefore, when executing the numerical algorithm, we always choose only one (positive) sign.

We note that fluctuations in the level spacings with respect to the average value $1/\rho$ are studied in quantum-chaos theory. Because the average density of energy levels in a potential of form (10) increases with increasing $E_\perp$, the initial array of levels undergoes the expansion procedure in the range under study [2, 4]. The new array of levels has the unit average density ($\rho = 1$).

RESULTS AND DISCUSSION

The construction of Poincaré sections shows that the dynamics of the electron is completely regular for the states at the potential-well depth (10). This is due to weakness of the influence of neighbors of the central atomic chain on its potential, which leads to conservation of the projection of the orbital angular momentum on the chain axis together with the energy $E_\perp$ during motion of the electron. As $E_\perp$ increases, the moving electron can visit regions at the periphery of the elementary cell, where the influence of neighboring chains leads to significant violation of the axial potential symmetry, the consequence of which is motion chaotization (starting from an energy of $E_\perp = -14$ eV for the electron with $E_\parallel = 5$ GeV).

Region *1* in Fig. 2 stands out among the regions of regular motion. The motion in it is close to that in the central field. The presence of this region is traced in the entire range of energies of transverse motion under consideration, namely, from −14 eV (completely regular motion) to −12 eV (upper edge of the potential well); in this case, in the range of $E_\perp \geq -12.8$ eV, the contribution of this region becomes determinative (regular tori including regions of types *1* and *2* in the Poincaré graphs also exist for deeper levels).

It is this region where the regularity of motion admits simple and obvious interpretation. The perturbative influence of neighboring chains is negligibly small near the chain axis, which leads to approximate preservation of the orbital angular momentum. The centrifugal barrier appearing in this case "prevents" the particle "from approaching" regions where there is no angular-momentum conservation and motion chaotization is produced.

It turns out that the contribution of this region to the average density of levels is constant with a good accuracy in the entire range under discussion and is

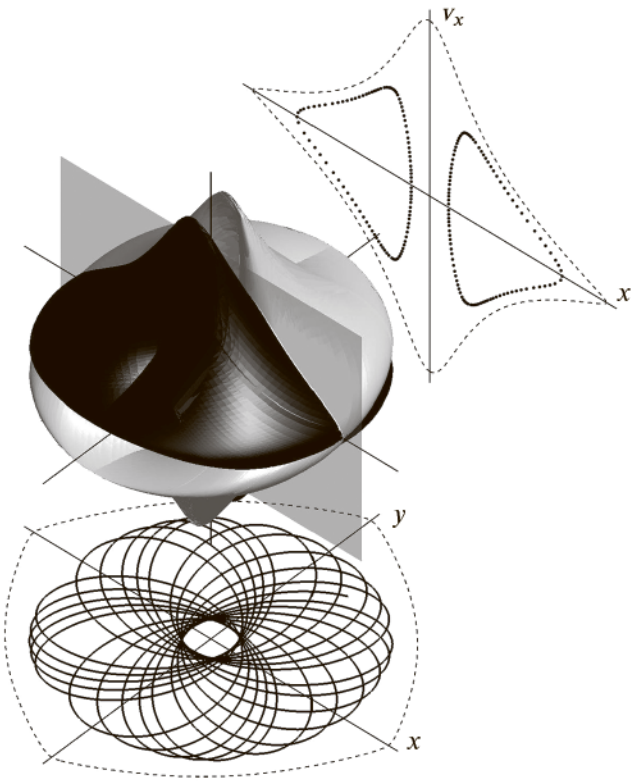

Fig. 3. Projection of two regions of phase space corresponding to a region of type *1* at the Poincaré section for three-dimensional space (x, y, v_x) (Fig. 2b). The cut plane (x, v_x), the Poincaré section, and the electron trajectory in the plane (x, y). are also shown. The light region corresponds to the counterclockwise orbital motion; and the dark one, to the clockwise one.

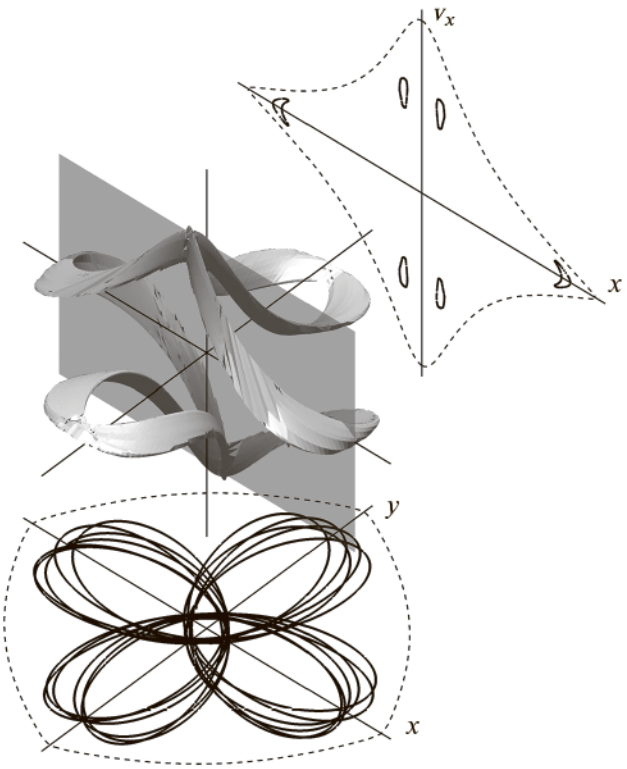

Fig. 4. Projection of a phase-space region of type *2* (corresponding to counterclockwise orbital motion) on the three-dimensional space (x, y, v_x) under the same conditions, as in Fig. 3.

approximately 34%. We emphasize that the Berry—Robnik—Bogomolny result (3) was obtained under the assumption that the contribution of the regions of regular motion to the level density is constant in the entire range under consideration. Thus, $\rho_1 = 0.34$ can serve as a lower estimate of the contribution of the regular-dynamics regions in the range

$$-12.82 \le E_\perp \le -12.08 \text{ eV}, \qquad (14)$$

where the contribution of this region becomes determinative. The average contribution of all regular regions is approximately $\rho_1 = 0.43$ in this range.

We note that two symmetric regions not intersecting in four-dimensional phase space and corresponding to motion in the given orbit clockwise and counterclockwise in the plane (x, y) correspond to the region of regular motion at a Poincaré section of each type, for example, of type *1*. However, projections of these regions on three-dimensional space (x, y, v_x) intersect, as shown in Fig. 3. In this case, in accordance with the foregoing in the discussion of formula (13), the corresponding contribution of levels related to regular motion to the density ρ_1 is determined by an integral of form (5) only by one of such two three-dimensional regions.

The form of an analogous three-dimensional region of type *2* (corresponding to counterclockwise motion) is shown in Fig. 4.

The quasiclassical energy-level density of an electron with an energy of $E_\parallel = 5$ GeV channeled in the Si crystal [100] direction was calculated in accordance with formula (5) by means of the Monte Carlo method. It is shown in Fig. 5 by a solid line; and the estimate of the contribution of regular-motion regions to it, by points. The error of this estimate is due to the difficulty in precisely determining the boundaries of the regular-motion regions and to that in taking into account contributions of small (in volume) regular-motion regions, the appearance of which accompanies the destruction of invariant tori at the interface between regions of regular and chaotic dynamics.

Figure 6 shows the distribution of level spacings for four types of nondegenerate energy levels of the transverse motion of an electron with a longitudinal-motion energy of 5 GeV in the range (14). In Fig. 6, the solid line denotes the Berry—Robnik—Bogomolny distribution with $\rho_1 = 0.3428$ (the heavy dashed line;

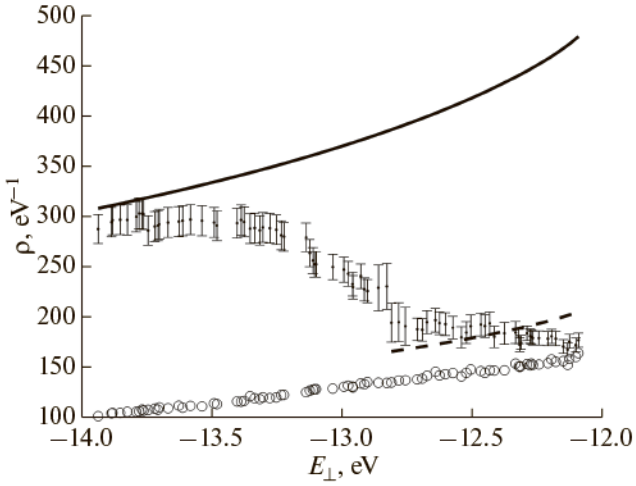

Fig. 5. Average energy-level density of transverse motion (the solid line) and the contribution of regions of type *1* to it (circles), and also the total contribution of all regular-motion regions (points; the error is due to the difficulty in precisely determining the boundaries of the regular-motion regions). The dashed line denotes the average density of energy levels related to regular-motion regions in the range (14).

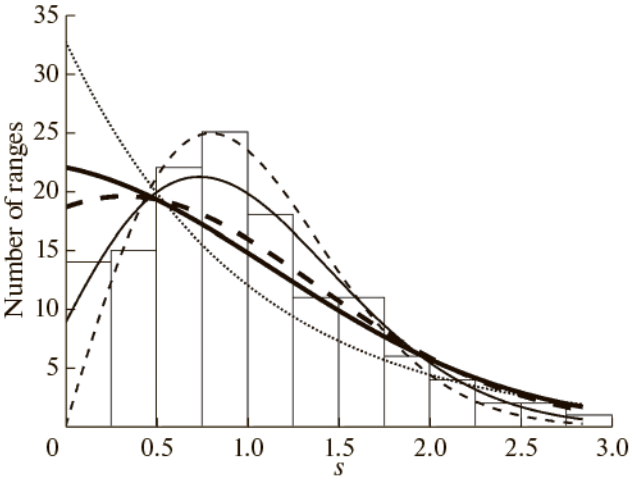

Fig. 6. Distribution of level spacings in region (14). The heavy solid line denotes the Berry–Robnik–Bogomolny distribution for $\rho_1 = 0.4274$; the heavy dashed line, the same for $\rho_1 = 0.3428$; and the thin solid line, the same for $\rho_1 = 0.1450$, estimated as a result of fitting using the maximum likelihood criterion. The thin dotted line corresponds to distribution (2); the thin dashed one, to distribution (1).

in this case, χ^2 is 8.7225) and $\rho_1 = 0.4274$ (the heavy solid line, $\chi^2 = 12.9508$). In both cases, we see that the Berry–Robnik–Bogomolny distribution describes the real distribution of level spacings better than distributions (1) (the thin dashed line, $\chi^2 = 17.9184$) and (2) (the dotted line, $\chi^2 = 30.8545$). However, fitting using the maximum likelihood criterion with ρ_1 as a free parameter leads to a value of about 15% (the thin solid line, $\chi^2 = 3.5489$), which is much smaller than the real contribution of the regular trajectory region to the level density in the range under consideration. The appearing discrepancy is due to the fact that the Berry—Robnik—Bogomolny distribution assumed that the chaotic and regular regions of phase space generate two independent sequences of levels, neglecting correlations between them.

CONCLUSIONS

In the paper, we have considered the channeling of 5-GeV electrons near the [100] chains of a Si crystal. It was shown that, near the upper edge of the potential well formed by the continuous potential of the atomic chain, the influence of neighboring chains leads to the appearance of a significant region of chaotic dynamics in the phase space of transverse electron motion.

Within the framework of the quasiclassical approximation of quantum mechanics, we calculated the energy-level density of transverse electron motion and determined the contribution of regular-motion regions retained in the upper part of the potential well to it.

The value of the relative contribution of the regular-motion regions to the level density is contained in the Berry—Robnik—Bogomolny distribution as an example of a parameter; this distribution describes the statistics of the level spacings of a quantum system, the classical analogue of which has partly regular dynamics and partly chaotic dynamics. It is established that, in the case of the channeled electron under study, the Berry—Robnik—Bogomolny distribution describes the statistical properties of nondegenerate energy levels better than the pure Poisson and Wigner distributions. However, the Berry—Robnik—Bogomolny distribution does not take a series of peculiarities of the system dynamics into account. In this context, it can be expected that the Podolskii—Narimanov distribution [15], taking tunneling accompanied by chaos into account, will describe the actual distribution of energy levels of transverse electron motion better at small level spacings.

REFERENCES

1. M. V. Berry, Proc. R. Soc. London, Ser. A **413,** 183 (1987). https://doi.org/10.1098/rspa.1987.0109
2. O. Bohigas and M. -J. Giannoni, Lect. Notes Phys. **209,** 1 (1984).
3. H.-J. Stöckmann, *Quantum Chaos: An Introduction* (Cambridge Univ. Press, Cambridge, 2000; Fizmatlit, Moscow, 2004).
4. L. E. Reichl, *The Transition to Chaos: Conservative Classical Systems and Quantum Manifestations*, 2nd ed.

(Springer, New York, 2004; RKhD, Moscow–Izhevsk, 2008).

5. A. I. Akhiezer and N. F. Shul'ga, *High-Energy Electrodynamics in Matter* (Nauka, Moscow, 1993; Gordon and Breach, Luxembourg, 1996).
6. A. I. Akhiezer, N. F. Shul'ga, V. I. Truten', et al., Phys.–Usp. **38** (10), 1119 (1995).
7. N. F. Shul'ga, V. V. Syshchenko, A. I. Tarnovsky, and A. Yu. Isupov, J. Surf. Invest.: X-ray, Synchrotron Neutron Tech. **9** (4), 721 (2015). https://doi.org/10.1134/S1027451015040199
8. N. F. Shul'ga, V. V. Syshchenko, A. I. Tarnovsky, and A. Yu. Isupov, Nucl. Instrum. Methods Phys. Res., Sect. B **370,** 1 (2016). https://doi.org/10.1016/j.nimb.2015.12.040
9. N. F. Shul'ga, V. V. Syshchenko, A. I. Tarnovsky, and A. Yu. Isupov, J. Phys.: Conf. Ser. **732,** 012028 (2016). https://doi.org/10.1088/1742-6596/732/1/012028
10. M. V. Berry and M. Robnik, J. Phys. A: Math. Gen. **17,** 2413 (1984). https://doi.org/10.1088/0305-4470/17/12/013
11. E. V. Bogomol'nyi, JETP Lett. **11** (2), 55 (1985).
12. M. D. Feit, J. A. Fleck, and A. Steiger, J. Comput. Phys. **47,** 412 (1982).
13. N. F. Shul'ga, V. V. Syshchenko, and V. S. Neryabova, J. Surf. Invest.: X-ray, Synchrotron Neutron Tech. **7,** 279 (2013). https://doi.org/10.1134/S1027451013020183
14. L. D. Landau and E. M. Lifshits, *Course of Theoretical Physics, Vol. 3: Quantum Mechanics: Non-Relativistic Theory* (Pergamon Press, Oxford, 1977); Fizmatlit, Moscow, 2016).
15. V. A. Podolskiy and E. E. Narimanov, Phys. Lett. A **362,** 412 (2007). https://doi.org/10.1016/j.physleta.2006.10.065